Optogenetic control of skeletal muscle activation during early postnatal growth induces expansion of the growth plate

Moaid Shaik[1,2], Nicole Migotsky[1], Lavi Coren[1,3], Nathan Chervin[1], Adam C. Abraham[1], Peleg Hasson[3], Megan L. Killian[1,2]
[1]University of Michigan, Ann Arbor, MI, USA; [2]Michigan State University, East Lansing, MI, USA; [3]Technion Israel Institute of Technology, Haifa, Israel
Email of Presenting Author: moaidshaik@gmail.com

Disclosures: Moaid Shaik (N), Nicole Migotsky (N), Lavi Coren (N), Nathan Chervin (N), Adam C. Abraham (ORS Membership Committee Chair), Peleg Hasson (N), Megan L. Killian (ORS Board of Directors)

Introduction: Musculoskeletal development is heavily influenced by mechanical forces generated from muscle contractions, particularly during early growth phases. These forces play a crucial role in shaping bone architecture and joint congruency. During normal growth, muscle activity is essential for proper endochondral ossification, joint cavitation, and skeletal morphogenesis. Disruption of these forces has been associated with altered bone growth and joint malformations. Much of this is known following loss of muscle contractions, yet the role of controlled and localized muscle activity during specific windows of early postnatal life is less defined. To address this knowledge gap, we employed in vivo optogenetic tools to induce controlled muscle contractions in neonatal mouse hindlimbs during early stages of postnatal development. By comparing stimulated limbs with contralateral non-stimulated controls, we aimed to determine whether unilateral muscle activation would drive detectable structural changes in the growing mouse skeleton.
Methods: All studies were approved by institutional IACUC. Acta1Cre;Chr2$^{LSL/LSL}$ (Cre+) and Chr2$^{LSL/LSL}$ (Cre-) pups were stimulated for 6 consecutive days starting at birth (P0 to P5) and euthanized at either postnatal day 7 (P7) or P10 (P10). Mice were genotyped as Cre+ if muscle contraction was observed after exposure to blue light. Upon Cre-recombination, the stop codon is removed and Cre+ mice express Channelrhodopsin-2 (ChR2), a membrane-bound light-activated cation channel. For optogenetic muscle stimulation, the mouse torso and head were covered with opaque nitrile material to expose the left hindlimb while also keeping the right hindlimb covered. Mice were stimulated using a 470nm, 3W LED (2000mA, Thor Labs SOLIS-470C) for 60 consecutive cycles (each cycle: 10x70ms on/30ms off pulses with a 4 sec pause between pulse cycles). At P7 and P10 (n=4 per group), mice were euthanized and hindlimbs were dissected, fixed in 4% paraformaldehyde (PFA), scanned using nanocomputed tomography (nanoCT), and processed for paraffin histology. Hindlimbs from stimulated (left) and non-stimulated (right) limbs were imaged using nanoCT (nanotom, phoenix|xray) to obtain high resolution three-dimensional images (7.9 micrometer voxel size; 80kV; 400mA; 0.762mm aluminum filter; average parameter of 3; and integration time of 500ms). Calibration phantoms containing air, water, and a hydroxyapatite mimic (1.69mg/cc; Gammex) were included in each scan. Dragonfly software (version 2024.1; Comet Technologies Inc.) was used to segment the tibia and fibula regions of interest (ROI). Otsu thresholding was used to segment bone from background noise prior to quantitative analysis of the full bone using a custom plugin to calculate length and trabecular (distal and proximal) and cortical (mid-diaphysis) bone morphometry. For P10 samples only, paraffin-embedded samples were sectioned at 5 µm in the sagittal plane and stained with Hematoxylin and Eosin (H&E) (StatLabs). H&E slides were imaged on a bright-field microscope (Cytation C10, BioTeck Agilent) at 4x magnification or higher and analyzed using QuPath (Bankhead et al., 2017). The distal tibial growth plate was imaged at 20x and cell count and tissue area were measured using the Stardist plugin (Schmidt et al., 2018) in ImageJ (Schindelin et al., 2012). ANOVA with repeated measures (bone morphometry only at P7 and P10 for left/right tibiae) or Welch's t tests (histology of P10 samples comparing left and right limbs) were conducted using GraphPad Prism. Both males and females were combined for analysis.
Results: Quantitative measurements of bone morphometry from nanoCT showed no significant differences in bone or total volumes between stimulated and non-stimulated limbs at P7 or P10. Similarly, tibial and femoral lengths did not differ significantly between limbs, indicating no detectable changes in longitudinal growth or mineralized bone mass with optogenetic stimulation. NanoCT analysis of the proximal and distal trabecular regions and mid-diaphysis cortical bone of the tibia further confirmed that there were no consistent differences in bone sub-compartments between stimulated and non-stimulated sides (data not shown). However, with histological examination, we found the distal tibial growth plate had localized differences in tissue morphology between stimulated and non-stimulated limbs at P10. Specifically, stimulated limbs had an expanded columnar zone of the growth plate compared to contralateral non-stimulated limbs (Fig1A, A'). This zone was characterized by increased height and a greater number of tightly aligned, flattened chondrocytes arranged in vertical columns (Fig1A, A'). In the stimulated limbs, the columnar region had more chondrocytes than contralateral non-stimulated controls (Fig1B, p=0.0785). Additionally, the columnar region was significantly larger in area compared to non-stimulated limbs (Fig1C, p=0.0072).
Discussion: This study showed that targeted optogenetic muscle activation during early postnatal development can induce localized expansion of the columnar zone of the growth plate by 10 days of age. This expansion did not yet affect overall mineralized tissue parameters. However, future work will explore if and how these soft tissue changes influence overall bone properties at advanced ages. These findings suggest that mechanical input from muscle contractions can modulate growth plate organization and size by potentially triggering chondrocyte proliferation or delaying progression to hypertrophy. Mechanical cues during the narrow postnatal window of accelerated skeletal growth may influence early stages of the chondrocyte maturation. Future work will assess whether extended stimulation results in accelerated endochondral ossification or increased longitudinal growth and whether these changes persist or normalize over time.
Clinical relevance: These findings highlight the significant contribution of muscle control during early postnatal development, a period when voluntary and independent movement is limited or absent. This work has important implications for populations with impaired mobility, whether caused by premature birth or neuromuscular dysfunction during critical developmental windows.

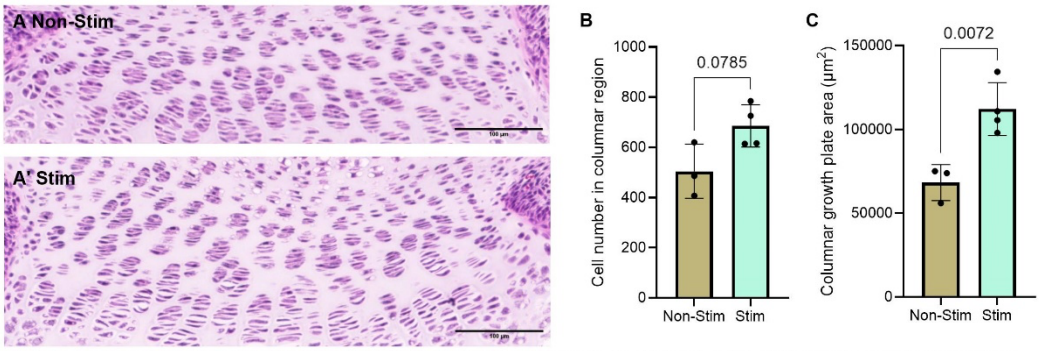

Figure 1. Histology and cell analysis of the columnar region in the distal growth plate of the tibia. (A) Representative histological images of the (A) non-stimulated limb and (A') stimulated limb, scale bar = 100µm. (B) Quantification of the number of cells in the columnar chondrocyte region and (C) total area of the columnar region of the distal growth plate.